

Article

Simulating Storm Surge Impacts with a Coupled Atmosphere-Inundation Model with Varying Meteorological Forcing

Alexandra N. Ramos Valle ^{1,*} , Enrique N. Curchitser ¹, Cindy L. Bruyere ² and Kathryn R. Fossell ²

¹ Department of Environmental Sciences, Rutgers University, New Brunswick, NJ 08901, USA; enrique@marine.rutgers.edu

² National Center for Atmospheric Research, Boulder, CO 80305, USA; bruyerec@ucar.edu (C.L.B.); fossell@ucar.edu (K.R.F.)

* Correspondence: alexandra.ramos@rutgers.edu; Tel.: +1-848-932-9800

Received: 14 February 2018; Accepted: 26 March 2018; Published: 5 April 2018



Abstract: Storm surge events have the potential to cause devastating damage to coastal communities. The magnitude of their impacts highlights the need for increased accuracy and real-time forecasting and predictability of storm surge. In this study, we assess two meteorological forcing configurations to hindcast the storm surge of Hurricane Sandy, and ultimately support the improvement of storm surge forecasts. The Weather Research and Forecasting (WRF) model is coupled to the ADvanced CIRCulation Model (ADCIRC) to determine water elevations. We perform four coupled simulations and compare storm surge estimates resulting from the use of a parametric vortex model and a full-physics atmospheric model. One simulation is forced with track-based meteorological data calculated from WRF, while three simulations are forced with the full wind and pressure field outputs from WRF simulations of varying resolutions. Experiments were compared to an ADCIRC simulation forced by National Hurricane Center best track data, as well as to station observations. Our results indicated that given accurate meteorological best track data, a parametric vortex model can accurately forecast maximum water elevations, improving upon the use of a full-physics coupled atmospheric-surge model. In the absence of a best track, atmospheric forcing in the form of full wind and pressure field from a high-resolution atmospheric model simulation prove reliable for storm surge forecasting.

Keywords: storm surge; hurricanes; ADCIRC; WRF; atmospheric forcing

1. Introduction

Tropical cyclones (TCs), and their associated storm surge, are some of the most damaging natural phenomena [1]. The magnitude of the resulting storm surge is dependent on geographical and bathymetric features, as well as TC characteristics including intensity, size, translational speed, and the direction in which the TC approaches the coast at landfall. The lack of availability of observations and accuracy of these properties prior to landfall, and the limitations in the characterization of the TC wind structure prove a challenge for real-time forecasting of storm surge impacts. When trying to understand how storm surge impacts will affect coastal regions, it is imperative to have a clear understanding of the factors that have influenced storm surge estimates in the past. Yet, as is the case with TCs, historical data on storm surge events is limited [2].

Based on a recent review on TC induced storm surges, maximum water level data is available for 389 TCs in the western North Atlantic Basin, with 17 events on Caribbean Islands, 242 events along the

U.S Gulf Coast and 110 events along the U.S. Atlantic Coast [3]. Only 22% of the events observed along the U.S Atlantic Coast occurred along the coastline from Virginia to Maine [3]. Some of these TC and extratropical cyclone (ETC) induced storm surge events have been highly destructive, partly because their landfall location has been around densely populated areas in states such as New York (NY) and New Jersey (NJ) [4]. In this study, we considered one of such events as a case-study. Hurricane Sandy is a TC known for its unique development and track, as well as the magnitude of the damages it caused. Despite being a unique case, Hurricane Sandy is an example of the vast impact TCs can have, and how a combination of factors can amount to such extensive damages [5]. As such, Hurricane Sandy is chosen as our case of interest.

Hurricane Sandy is now ranked as the fourth costliest storm to impact the US [6]. The damages produced were primarily caused by the large extent of the TC's wind field [7], the near perpendicular landfall angle [8], and the consequent storm surge produced by the combination of these factors. The storm surge observed reached up to 3.85 m above normal tide level at Kings Point, NY, USA [7,9]. Moreover, having reached unprecedented storm surge heights, Hurricane Sandy tested the resilience of the NJ and NY coastal infrastructure to storm surge. Events such as Hurricane Sandy highlight the importance of understanding the physical processes behind storm surge and improving modeling techniques, and as such, this remains an active topic of research.

Atmospheric forcing is the principal driver of storm surge [10,11]. In storm surge models, atmospheric forcing is provided in the form of surface pressure and near-surface wind fields from various sources and configurations. These can include the use of cyclone track-based data implemented in parametric vortex models, as well as the use of wind reanalysis products and 3D atmospheric models.

Parametric vortex models use a simple set of storm parameters to represent the wind and pressure fields. These models range in complexity in their representation of the TC wind field, which can be represented as a simple symmetric vortex [12] or can more accurately describe the wind field by accounting for wind asymmetries [13,14]. Some storm surge models such as the Sea, Lake and Overland Surges from Hurricanes (SLOSH) allow for the use of symmetric vortex models, with spatially constant radius of maximum wind (R_{max}), to characterize the TC wind field for a given track dataset. However, a recent study comparing multiple meteorological forcing for the case of Hurricane Rita found that due to uncertainties in the wind field, an asymmetric model outperforms the symmetric model in forecasting storm surge [15].

The parameters needed for implementation in the parametric vortex model include the storm location, minimum central pressure, maximum wind velocity and radius of maximum winds [10,11]. These parameters are available as part of the National Hurricane Center (NHC) forecast advisories issued every 6 h throughout the storm's lifetime. The availability of these storm parameters and the computational efficiency of parametric vortex models provide for timely storm surge forecasts. As such, the use of parametric vortex models is suitable for real-time forecasting of storm surge. However, these models are a simplification of the TC wind field and fail to capture important dynamic processes such as weakening and distortion of the TC wind field after interaction with topography. Full physics atmospheric models can more accurately represent these processes and interactions in the TC wind field and have been used for storm surge assessment. As storm surge modeling shifts into real-time coupling of inundation and full-physics atmospheric models, it becomes relevant to study and evaluate the coupled model performance in predicting storm surge. Understanding of the limitations of these coupled systems will contribute to further development in the field.

Recent studies have researched the effect of using various meteorological forcing for storm surge or wave assessment. Akbar et al. [15] performed a hindcast of Hurricane Rita to study the effect of varying wind fields on storm surge estimates, including meteorological forcing from the National Oceanic and Atmospheric Administration (NOAA)/Hurricane Research Division's (HRD) Real-time Hurricane Wind Analysis System (HWIND; [16]), the Dynamic Holland Model [12], and the Asymmetric Holland Model [14]. Results from the study indicate that HWIND performed better than both the Dynamic and Asymmetric Holland Models. The sensitivity of storm surge to different

meteorological forcing types for the case of Hurricane Isaac (2012) in the Gulf of Mexico has also been studied. Dietrich et al. [10] showed that provided availability of accurate forecast advisories, in a hindcast scenario, a parametric vortex model results in reasonable storm surge estimates. Bennett and Mulligan [17] compared the effect of wind fields from two parametric models and a 3D atmospheric model on the generation of surface waves by Hurricane Sandy and concluded that the 3D atmospheric model, which has the best description of the storm wind field, is most suitable for their assessment.

Studies comparing different atmospheric forcing make use of NHC forecast advisories or NHC-BT datasets in their parametric vortex model implementations, and compare them to storm surge forecasts forced by full-physics atmospheric models or wind reanalysis products (e.g., Akbar et al. [15], Dietrich et al. [10] and Bennett and Mulligan [17]). That is, the comparisons are not exclusive of atmospheric forcing method but also account for accuracy of the data used. In this study, we perform similar comparisons but aim to isolate the effectiveness of using a parametric vortex model in contrast to a full-physics atmospheric model. To achieve this, we explore the use of a single dataset produced by an atmospheric model and format the output according to the forcing method of interest. The surface pressure and near-surface wind fields from an atmospheric model are directly implemented as atmospheric forcing. In addition, we process the output of the atmospheric model to obtain a track file similar to the NHC-BT and implement it using the Generalized Asymmetric Holland Model (GAHM; [13]) described in Section 2.2. This method allows us to perform a more direct comparison between both atmospheric forcing configurations. The methodology of extracting a track dataset from a full-physics atmospheric model highlights an alternative way of incorporating these models for hindcasting and real-time forecasting purposes.

The model configurations, model coupling details and an overview of the simulations performed are described in Section 2. Results from the control simulation and the coupled model simulations are described in Section 3. The implications and limitations of the study are discussed in Section 4. Finally, conclusions are provided in Section 5.

2. Materials and Methods

2.1. WRF Model Configuration

Sixty-hour simulations of Hurricane Sandy, initialized at 0000 UTC on 28 October 2012, were performed using the Weather Research and Forecasting (WRF) model [18] version 3.8. Simulations initialized prior to this time result in significant storm track error at landfall. Similar results were reported in Galarneau et al. [19], where simulations of Hurricane Sandy initialized at 0000 UTC 23–27 October showed substantial track error at landfall. The spread of landfall locations extended between the Maryland/Delaware coast to the northern NJ and NY coastal area. Simulations were made using (i) a 12-km horizontal resolution domain that covered the western North Atlantic Ocean basin and the eastern US, (ii) a 4-km horizontal resolution domain with the same outer extent, and (iii) a two-way nested configuration with a 12-km horizontal resolution outer domain and a smaller, vortex following nest of 4 km. The simulations ran with 38 vertical levels and a model top at 50 mb. To allow for model stabilization and adjustment in the 12-4 km vortex-following simulation, the nested domain was prescribed to start tracking the vortex after 1 h of the simulation start time.

Initial and boundary conditions were provided by the European Centre for Medium-Range Weather Forecasts (ECMWF) ERA-Interim reanalysis data [20] and were updated every 6 h. The physical parameterizations implemented were those used by the National Center for Atmospheric Research's real-time hurricane simulations for domains comparable to the 12- and 4-km resolution used in this study. The parameterization schemes used include (Table 1): WRF Single-moment 6-class microphysics scheme [21], Yonsei University boundary layer scheme [22], Tiedke cumulus parameterization [23], RRTMG for shortwave and longwave radiation parameterization [24], and the NOAH land surface model [25]. The simulation was initialized with sea surface temperature (SST) values from ERA-Interim for 28 October 2012 0000 UTC and was not updated throughout the

simulation. The SST profile varied spatially but not temporally. Observed SST along the storm track remained approximately constant at around 25 °C until Sandy moved away from the Gulf Stream and towards the NJ coast and encountered cooler waters.

Table 1. Model configuration for Hurricane Sandy WRF 12-4 km, WRF 12 km and WRF 4 km simulations.

Model Parameter	Configuration
Time step (s)	60 ¹
Cumulus convection	Tiedke
Boundary layer	Yonsei University (YSU)
Microphysics	WRF single-moment 6-class scheme (WSM6)
Land surface	Noah land surface model
Radiation	Rapid Radiative Transfer Model for GCMs (RRTMG)

¹ Simulations ran with the same configuration except for the WRF 4 km with time step of 30 s.

The simulated cyclone track data, including the location, maximum wind speed and minimum pressure of the storm were directly output from WRF and used for model evaluation.

2.2. ADCIRC Model Description and Atmospheric Forcing Configuration

To hindcast the storm surge from Hurricane Sandy, WRF output was used as forcing for the two-dimensional depth integrated (2DDI) implementation of the ADCIRC hydrodynamic model [26,27]. ADCIRC has been used for various storm surge impact studies for cases in the Gulf of Mexico [10,28–30], along the eastern US coast [31] and more specifically for the NJ and NY coastal region [5,32–35]. ADCIRC uses a finite element unstructured triangular grid allowing for higher resolution near the coast and coarser resolution in the deep ocean. In this study, simulations were performed on a grid developed by the Federal Emergency Management Agency (FEMA) as part of the Region II Coastal Storm Surge Study [36]. The mesh domain of the FEMA grid is shown in Figure 1 and includes the U.S. Atlantic Coast, the Gulf of Mexico, and the Caribbean with higher resolution along the NJ and NY coastlines (inland spacing 80–500 m; 30 m in limited areas). This mesh was originally used for the case of Hurricane Sandy and has since been implemented in storm surge modeling studies for this case as well as other tropical and extratropical systems [33,37]. Details of the model configuration are described in Table 2.

Tides-only simulations were performed and initialized 10 days prior to the first time-record in the NHC-BT (23 October 0000 UTC) for the control simulation, and prior to the WRF initialization time (28 October 0000 UTC) for the WRF-ADCIRC simulations. This time difference results from a delayed initialization of the WRF simulations. Recall that for our case study, WRF simulations initialized earlier than 28 October 0000 UTC resulted in large track errors at landfall (Section 2.1). All simulations were forced with 7 tidal constituents: M2, N2, K2, S2, K1, O1, Q1 along the open boundary.

After the tides-only simulations, five 60 h simulations with meteorological forcing were carried out. The control ADCIRC simulation (CTL) was conducted with forcing provided from the 6-hourly NHC-BT data for Hurricane Sandy. Atmospheric forcing for CTL was implemented with the GAHM parametric model. Given that the NHC-BT dataset is a post-storm analysis, CTL estimates of water elevation are considered the closest to truth or observed values.

The CTL experiment was followed by four WRF-ADCIRC simulations. The four WRF-ADCIRC simulations are characterized as follows (Table 3): (i) forcing with hourly Simulated Cyclone Track (SCT) data from the outer domain of the two-way nested WRF 12-4 km simulation (SCT12-4), (ii) forcing with 3 h Full Wind and Pressure fields (FWP) from the WRF 12-4 km simulation (FWP12-4), (iii) forcing with 3 h full wind and pressure fields from the WRF 12 km simulation (FWP12), and (iv) forcing with 3 h full wind and pressure fields from the WRF 4-km simulation (FWP4).

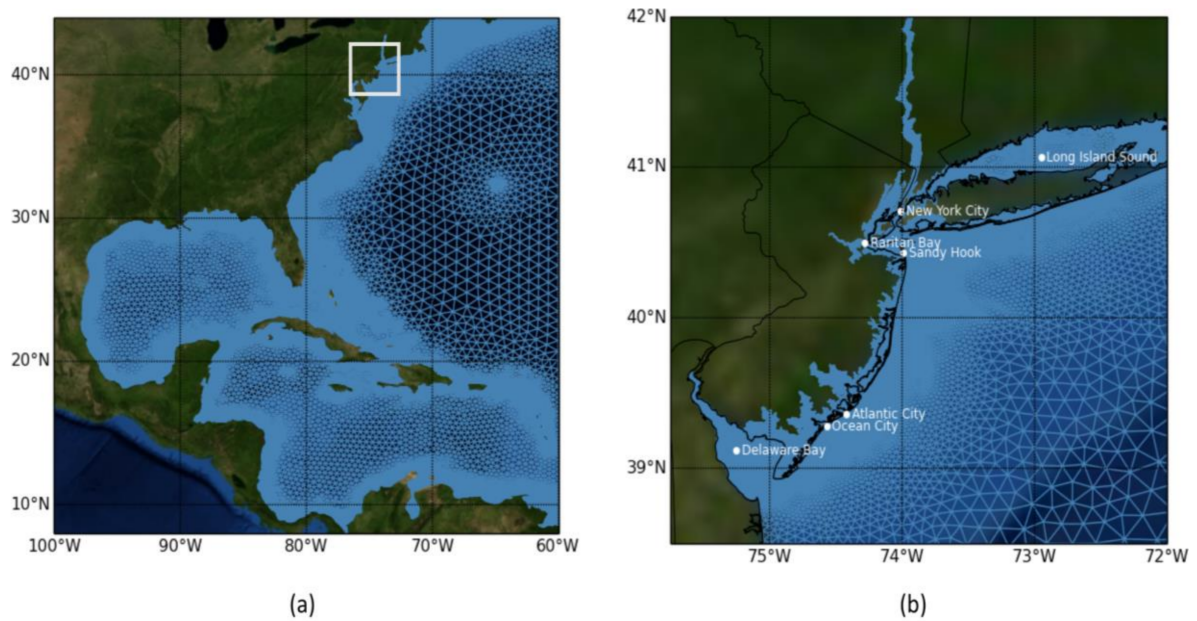


Figure 1. (a) Advanced Circulation Model (ADCIRC) finite element unstructured mesh used for the Federal Emergency Management Agency (FEMA) Region II Coastal Surge Study [36]. The mesh has been designed with higher resolution along the Hudson Bay, NJ, and NY coastal regions. The mesh has 604,790 nodes; (b) Zoom in for the white box in (a) of the NJ and NY coastline. Raritan Bay, Delaware Bay and Long Island Sound bays are identified.

Table 2. ADCIRC model configuration parameters.

Parameter	Description	Value
NOLIBF	Bottom stress	1; quadratic bottom friction law
NCOR	Coriolis parameter	1; spatially variable
NWS	Atmospheric forcing	20; Generalized Asymmetric Holland Model format 12; forcing in rectangular grid format
NRAMP	Ramp option parameter	1; hyperbolic tangent ramp function
DRAMP	Days to apply ramp function	7 days

Table 3. Description of meteorological forcing for each coupled simulation.

Case	Forcing	Source
CTL	Best track	NHC
SCT12-4	Simulated cyclone track	D01 from WRF 12-4 km
FWP12-4	Full wind and pressure fields	WRF 12-4 km
FWP12	Full wind and pressure fields	WRF 12 km
FWP4	Full wind and pressure fields	WRF 4 km

The SCT12-4 simulation is comparable to the CTL simulation but includes a different atmospheric forcing source. The SCT12-4 simulation is forced with cyclone track data obtained from the 12-4 km nested WRF simulation, for which the forcing is applied through a parametric vortex model. Prior to implementing the track-based meteorological forcing into ADCIRC, WRF data is processed to recalculate track data. In addition, wind structure information is calculated since the WRF model output does not explicitly contain this information. Wind structure data obtained from post-processing include the radius of maximum winds (Rmax) and the wind radii for the 34-, 50- and 64-kt isotachs.

Wind radii for each isotach is obtained by calculating the weighted average with respect to the diagonal in each of the quadrants.

Since TCs often exhibit asymmetries in their structure, in this study, we use the implementation of ADCIRC which allows the use of an asymmetric model to characterize the wind field in the CTL and SCT12-4 simulations. The model used is the GAHM, which is an adaptation from the asymmetric Holland model [12] but modified to use information from all available isotachs. Wind structure information includes the radius of maximum winds for the 34-, 50- and 64-kt isotachs. Gao et al. [13] and Dietrich et al. [10], provide a comprehensive description of the parametric vortex model implementation. In the following we provide an overview of the atmospheric forcing implementation. GAHM, built-in within ADCIRC, is used to model the TC wind and pressure fields. It calculates the wind velocity and surface pressure at each mesh node, directly coupling to ADCIRC. GAHM is designed to fit multiple isotachs in each of the four storm quadrants and as such produces a hurricane vortex with spatially varying R_{max} [13]. The use of multiple isotachs provides for a better representation of the full wind field and of the TC wind field asymmetries.

The three remaining simulations (FWP12-4, FWP12, and FWP4) are forced with the 10 m wind and surface pressure field outputs from WRF simulations. The wind and atmospheric pressure fields are spatially interpolated onto the ADCIRC model domain and temporally interpolated to correspond with the model time step.

3. Results

The WRF-ADCIRC simulations were compared to CTL, and to water elevation observations at various stations. The FWP12-4 simulation was directly compared to SCT12-4 to determine differences arising from the use of varying meteorological forcing methods. Finally, a sensitivity test based on model resolution was performed for the simulations forced with the full-physics atmospheric model.

3.1. WRF Model Evaluation

Prior to the WRF-ADCIRC coupling the accuracy of the simulated TC was evaluated. Evaluation of the WRF model simulations were performed by comparing the track and intensity of the simulated storms with data from the NHC-BT dataset. The discussion will be focused mainly on the WRF 12-4 km simulation, except in situations that warrant further analysis.

The two-way nested WRF 12-4 km model simulation proved skillful in predicting the observed track and landfall location. At the time of initialization, the simulated storm track was located about 46 km to the right of the observed BT location (Figure 2). The track error increased to a maximum of about 110 km, with the simulated track shifting to the left of the observed location on 29 October 0600 UTC. The track then followed the same trend as the NHC-BT observations and took Hurricane Sandy's characteristic Northwest turn towards the NJ coast. After 29 October 1600 UTC, the track error was reduced to about 32 km. The simulated storm remained to the left of the observed track and made landfall south of Brigantine, NJ, USA with a track error at the time of landfall at 2330 UTC on 29 October of 21.5 km (Figure 2).

In terms of the minimum sea level pressure at landfall, the simulated hurricane was only fractionally weaker (3.6 mb) than the observed. The lifetime minimum pressure obtained by our simulation was 948.5 mb at 0000 UTC 30 October, while the observed hurricane reached a minimum pressure of 940 mb at 1800 UTC 29 October. The slightly weaker nature of the simulated storm is evident when comparing the maximum winds (Figure 3). The maximum wind of the simulated storm at landfall was 4.48 ms^{-1} less than observations, but the error is still within the range of NHC's annual average intensity error for a 48 h forecast of about 5.45 ms^{-1} (10.6 kts per 2016 standards; [38]). Despite the weaker maximum wind at landfall, our simulation reached the secondary intensity peak of 43.5 ms^{-1} which nearly matches the observed maximum of 44 ms^{-1} . The simulated storm reached its maximum early at 0600 UTC on 29 October, which is approximately 6 h prior to the observed peak for Hurricane Sandy.

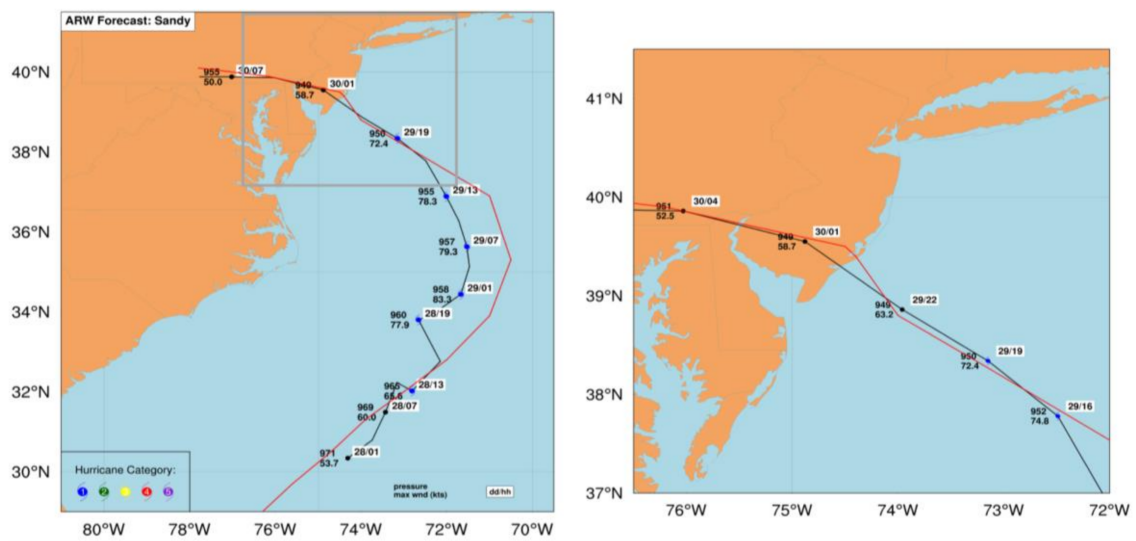


Figure 2. The Weather Research and Forecasting (WRF) model 12-4 km simulated hurricane Sandy track (black) initialized on 28 October 0000 UTC compared to National Hurricane Center (NHC) best track data (red). The simulated storm makes landfall on 30 October at 0000 UTC about 20 km south of hurricane Sandy’s landfall location near Brigantine, NJ, USA. Track information is provided every 6 h. Insert: zoom in view of cyclone landfall location with track information provided every 3 h.

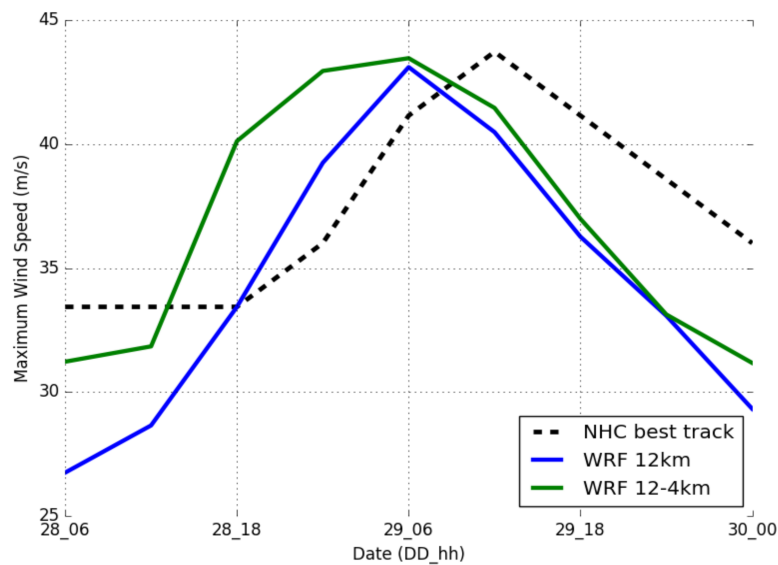


Figure 3. Cyclone wind speed from NHC best track (dashed black line); WRF 12 km simulation (blue); and WRF 12-4 km simulation (green).

The single-nested WRF 12 km simulation on the other hand, followed the general observed track but showed signs of instability along the track, prior to recurving to the left (Figure 4). The track error is less than that of the WRF 12-4 km simulation in the hours prior to landfall but increases to about 37 km as it approaches the coast and makes landfall north of the observed location. The WRF 12 km simulated TC was in general weaker than the WRF 12-4 km. In this case, the lifetime minimum pressure occurring near landfall on 30 October 0100 UTC, was 949.8 mb. The storm also reached a maximum intensity of 43.1 ms^{-1} on 29 October at 0600 UTC. As shown in Figure 3, the storm starts with a lower intensity than the WRF 12-4 km simulated TC, remaining as such for the entire simulation until reaching peak intensity and weakening faster than the former after landfall.

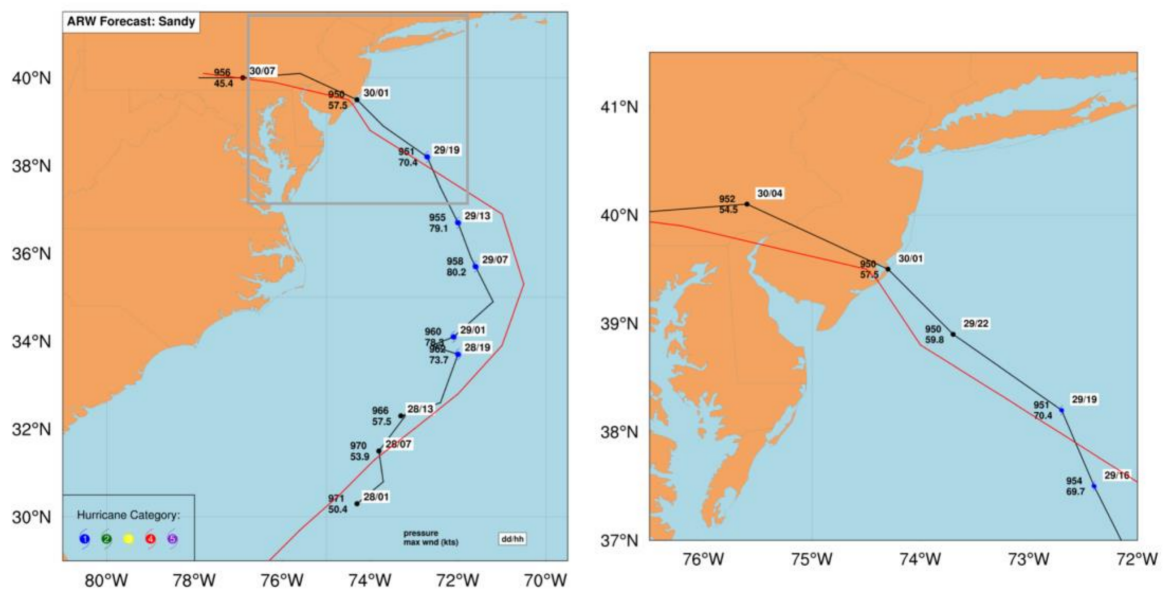


Figure 4. Same as Figure 2 except track is presented for the WRF 12 km simulation.

Wind patterns and minimum pressure estimates were further explored for the WRF 12-4 km simulation by comparing observations from the NOAA National Data Buoy Center buoys and weather stations along the coast of NJ and NY to the WRF simulations (<http://www.ndbc.noaa.gov/>). Nevertheless, the comparisons provide additional insight into the WRF 12-4 km simulated wind and pressure field patterns. Unlike many stations in the vicinity, the New York Harbor Entrance Station recorded wind and pressure data throughout the entire analysis period (Figure 5f). The simulated pressure pattern matched well with observations and accurately captured the pressure drop at the buoy, with a significant correlation coefficient of 0.995. The simulated wind patterns followed the same general behavior as the observed winds, although the simulated winds appear to be slightly overestimated at this station (correlation of 0.952). Other stations examined followed a similar pattern of significant correlation between pressure and wind estimates. Minimum pressure was well simulated in all stations (Figure 5). Wind speed time series for the Cape May, NJ and Kings Point, NY stations (Figure 5d–e) showed more discrepancies. In these stations the simulated winds are overestimated, however the peak wind speed is accurately captured in the Cape May station.

For storm surge assessment, it is important that the atmospheric simulations can reproduce the structure and location of maximum intensity observed for TCs, but more so it requires that the overall wind fields are accurately depicted (i.e., extent and asymmetries). We compared the wind field from the HWIND product for various forecast times before and during landfall to the WRF 12-4 km simulation. We determined that the WRF 12-4 km simulation could capture the main features in structure and intensity observed for Hurricane Sandy, with maximum wind intensities both on the left and right side of the track, characteristic of extratropical cyclones. Our comparison shows that at 2100 UTC 29 October, 2 h prior to landfall, the model simulation reproduced the annular/semi-annular structure of the TC, as well as the location and intensity of the maximum winds in the lower TC quadrants (Figure 6). After landfall at 0000 UTC 30 October, the model simulation was also able to capture the weakening and dissipation of the TC as it started losing definition of its structure when interacting with land and topography.

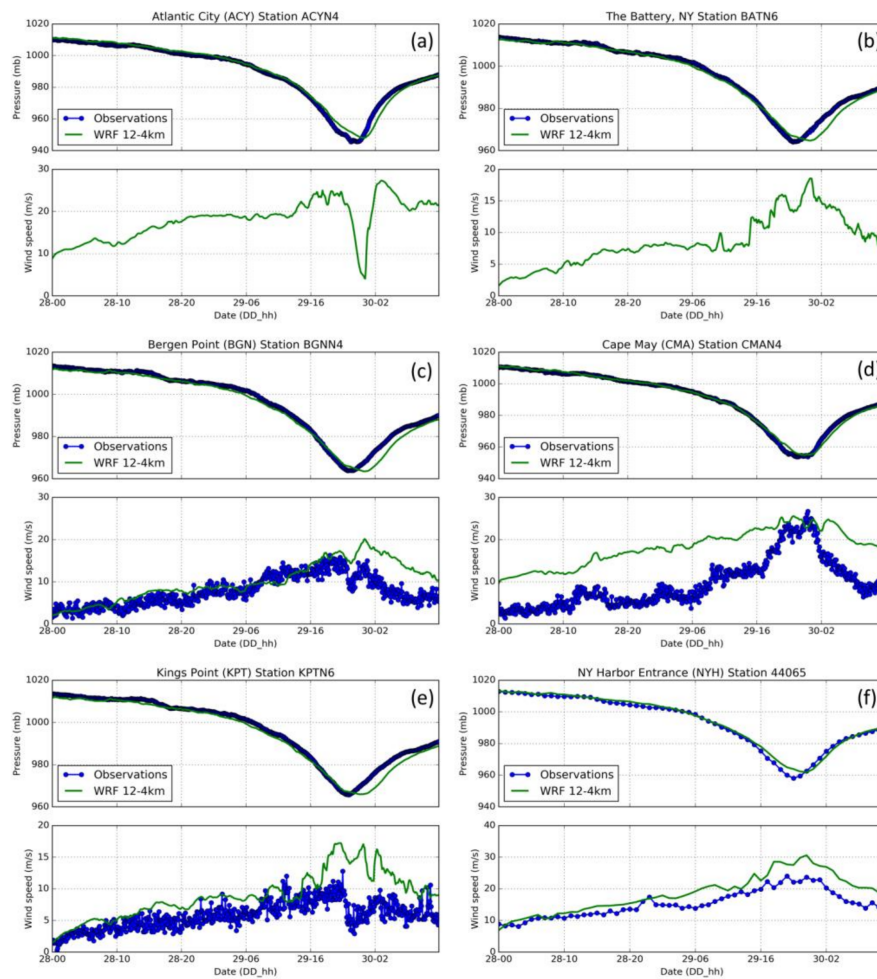


Figure 5. Comparison of WRF 12-4 km simulated minimum pressure (top) and maximum wind (bottom) estimates with station observations for (a) Atlantic City, NJ, (b) The Battery, NY, (c) Bergen Point, NY, (d) Cape May, NJ, (e) Kings Point, NY and (f) New York Harbor Entrance, NY stations.

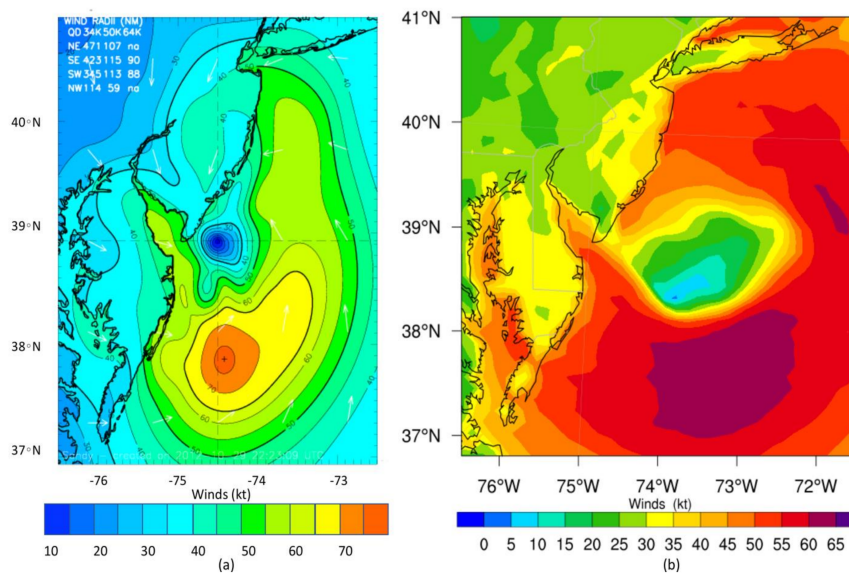


Figure 6. Wind field analysis for 2100 UTC 29 October 2012 from (a) HWIND (source: NOAA/AOML/Hurricane Research Division); (b) WRF 12-4 km simulation.

3.2. Control Storm Surge Simulation

Figure 7 shows the maximum water elevation for the CTL run, where ADCIRC was forced with the NHC-BT data for Hurricane Sandy and implemented with the GAHM. The NHC-BT should have marginal track and intensity errors, and per ADCIRC model configuration, should be the closest representation to actual observations. In the WRF12-4 km simulation of Hurricane Sandy strong winds prevail on both sides of the storm tracks, as discussed in Section 3.1. The maximum water elevation estimates reached the maximum observed storm tide (storm surge + tide) of about 4 m. High water elevations are observed in areas right of the storm track including the NY Harbor and Long Island Sound regions. Opposite results are seen to the left of the storm track, where storm surge was lowest overall. Maximum water elevation estimates on the southern coast of NJ and in the Delaware Bay range between 1–2 m. Near Brigantine and Atlantic City water elevation estimates were moderate, ranging between 1.5 and 2.5 m.

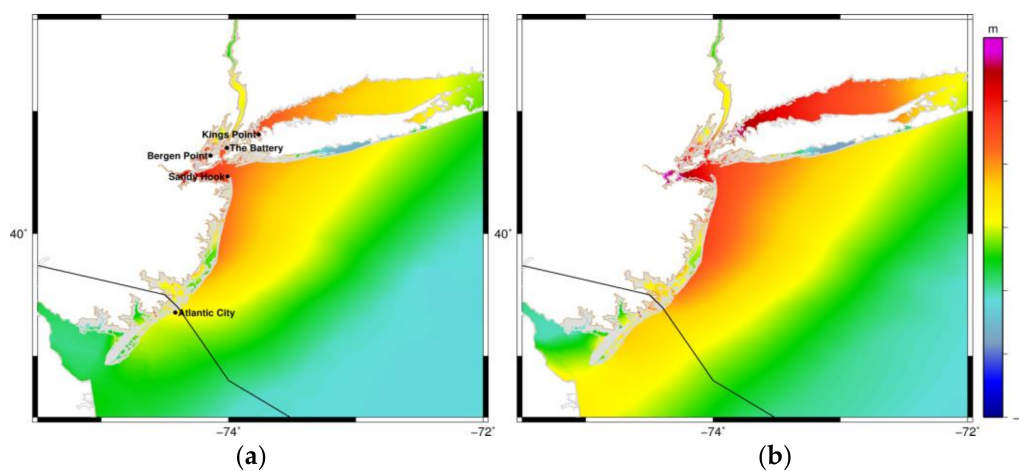


Figure 7. (a) Simulated maximum water levels above mean sea level (MSL) during the period of 23 October 0000 UTC through 30 October 1200 UTC for the CTL ADCIRC run forced with the NHC best track dataset. (b) Same as (a) except simulation is initialized on 28 October 0000 UTC to correspond with initialization period of WRF simulations. The black line indicates the track of Hurricane Sandy as it made landfall in New Jersey north of Atlantic City.

3.3. WRF Simulated Cyclone Track-Forced Storm Surge Simulation

The WRF-ADCIRC SCT12-4 simulation results show maximum water elevation estimates that do not reach the maximum observed storm tide for Hurricane Sandy (Figure 8a). One of the causes to consider is the simulated TC size. On 28 October 0000 UTC the NHC-BT data indicate that Hurricane Sandy's 34-kt wind radii extent for the NE, SE, SW and NW quadrants are 480, 300, 300 and 280 nm, respectively. The 34-kt wind radii calculated for SCT12-4 were generally smaller than observations, particularly in the NE quadrant, with a 241-, 276-, 298- and 326-nm extent for the NE, SE, SW, and NW quadrants, respectively. The simulated storm in SCT12-4 is smaller than was observed for Hurricane Sandy and is not expected to have that significant of an effect on maximum water elevations.

Water elevation in the NY Harbor, Raritan Bay and Long Island Sound areas mainly ranged between 2 and 3 m, while estimates in the Delaware Bay were lower and ranged between 1 and 2 m. When compared to the CTL run, the simulated maximum elevation gradient resembles that of the CTL, with highest surge in the NY Harbor and Long Island Sound regions. However, the maximum water elevation estimate in the NY Harbor was largely underestimated by the SCT12-4 simulation with differences ranging between about 0.75 and 1.5 m (Figure 8b). SCT12-4 overestimates maximum water elevation in the Delaware Bay. Near the area of landfall in Brigantine, NJ the differences between the CTL and SCT12-4 are the lowest. Differences range between 0.0 and -0.5 , owing to similarities

in track and intensity between the WRF12-4 simulated storm and observations for Hurricane Sandy near landfall.

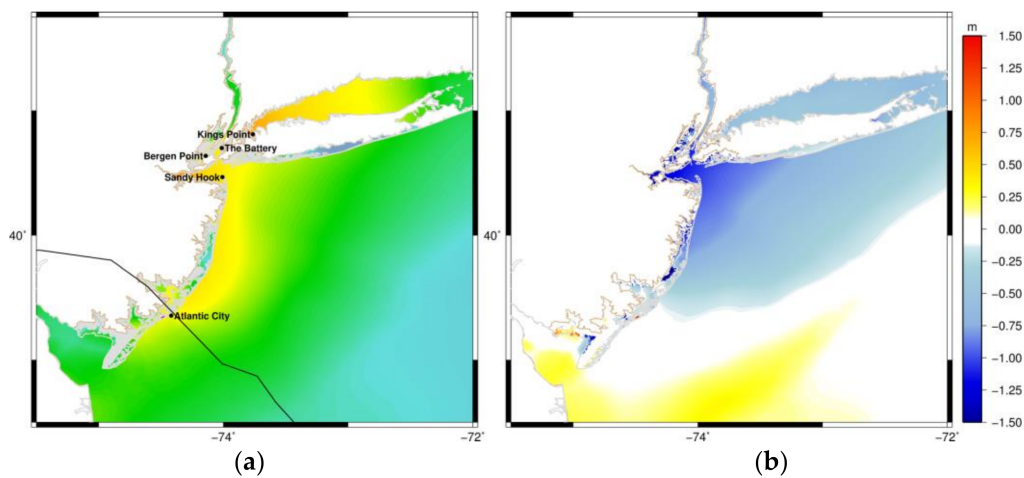


Figure 8. (a) Simulated maximum water levels above MSL during the period of 28 October 0000 UTC through 30 October 1200 UTC for SCT12-4. The black line represents the track of the storm, which makes landfall closer to Atlantic City, south of the observed landfall location. (b) Difference between SCT12-4 and the control simulation.

3.4. WRF Full Field-Forced Storm Surge Simulations

One of the main features evident in the FWP12-4 simulation, is high maximum water elevation in Long Island Sound (Figure 9a), where maximum water elevations in this region reached up to 4 m, overestimating CTL by about 1 m. Compared to CTL, the FWP12-4 simulation underestimates the maximum water elevation along the NY Harbor and Raritan Bay areas by about 0.4–1.0 m (Figure 10a), as expected for a storm with winds between 5 and 8 m/s weaker than observations. Meanwhile it overestimates water elevations by about 0.4 m in the coastal region south of Atlantic City, NJ, USA.

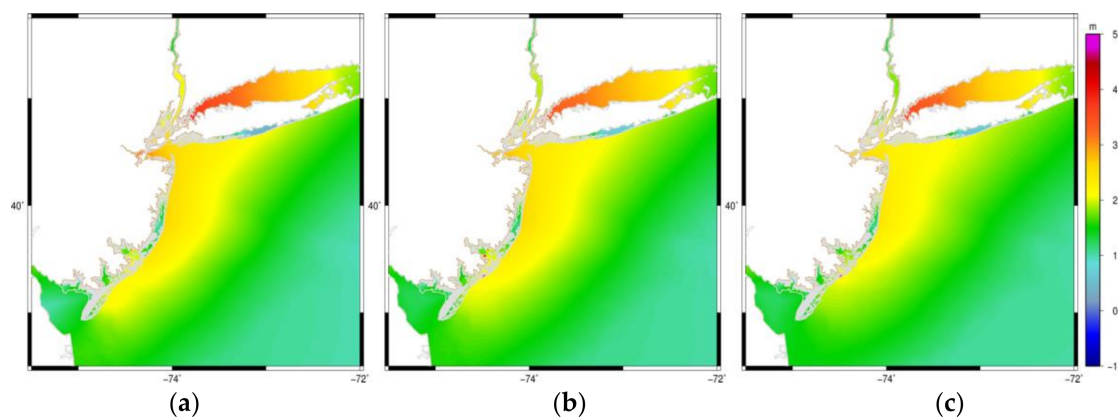


Figure 9. Simulated maximum water levels during the period of 28 October 0000 UTC through 30 October 1200 UTC for (a) FWP12-4; (b) FWP12; and (c) FWP4.

The area where the maximum water elevation ranged between 2 and 3 m is broader in this simulation, extending further east into the Atlantic Ocean than in the SCT12-4 simulation. This area of higher water elevation also extends further south along the NJ coastline in FWP12-4 than both the CTL and SCT12-4 simulations, pointing to a larger TC wind field representation in the full-physics model compared to the parametric wind model. Also, evident in this simulation are higher estimates

along the Hudson River where the maximum water elevation reached above 2 m. The increased surge along the Hudson River is a feature that could not be captured in the previous track-forced simulation (SCT12-4) but is present in the CTL run. These discrepancies could point to significant differences in wind speed and direction along the narrow river.

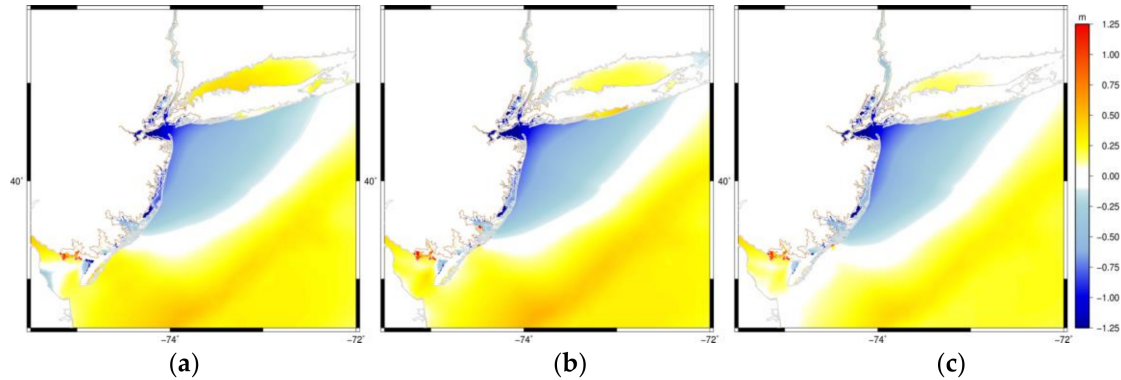


Figure 10. Differences from the control simulation for the (a) FWP12-4; (b) FWP12; and (c) FWP4 simulations.

The sensitivity of storm surge estimates to differences in horizontal resolution of the meteorological input data in the form of full wind and pressure fields were also explored. The FWP12 produces similar maximum water elevation estimates when compared to the FWP12-4. Maximum water elevation for FWP12 are generally lower than FWP12-4 in the New York Harbor and Long Island Sound region. When comparing FWP12 to the CTL, differences are reduced in Long Island Sound (Figure 10b). A similar maximum elevation pattern is observed for FWP4, where maximum elevations in Long Island Sound compare closer to the CTL with differences around 0.3 m (Figure 10c). However, FWP4 underestimates water elevations in the NY Harbor region by 1.2–2.0 m.

3.5. Inter-Comparison of Simulations with Varying Meteorological Forcing

All simulations exhibit higher storm tide to the right of the TC track, and a lower storm tide estimate to the left of track. This result is expected for TCs with wind maxima on the right-hand side of the storm. The fact that ETCs can exhibit two regions of wind maximum on either side of the track has notable implications for this case. With strong offshore winds to the left of the track, more water is moved offshore, reducing storm surge on the left side of the track. Observations, as well as all model simulations, show this pattern of higher storm tide along the northern NJ coast and Long Island (right of track), and lower estimates along the southern NJ coast (left of track).

Figure 11 shows the difference in modeled maximum water elevation between SCT12-4 and FWP12-4. Results indicate that much of the difference observed between these simulations is within Long Island Sound. In this region, FWP12-4 estimates water elevations that are generally between 0.8 and 1.0 m above the SCT12-4 estimates. Meanwhile, the opposite is observed in the Delaware Bay, where SCT12-4 estimates a storm surge about 0.4 m higher than FWP12-4, pointing to possible differences in wind field extent. Overall, differences were within the 1 m range, with FWP12-4 overestimating maximum elevation in most of the area of study, when compared to SCT12-4. Nevertheless, the track-forced SCT12-4 simulation had higher correlation and lower RSME than the FWP12-4 simulation.

We then compared all simulations to maximum water elevation hourly time series from various NOAA Tides and Currents [39] stations marked on Figure 7. Results point to a reduction in the extent of the inundation area, as discussed in results from Akbar et al. [15]. Out of the seven stations considered, three stations are projected to be dry, one station is projected to dry after initial inundation, and 3 others are wet throughout the entire simulation. These three stations are discussed here and

include Atlantic City, NJ station (ID: 8534720), The Battery, NY station (ID: 8518750) and Montauk, NY station (ID: 8510560). Results from the time series comparisons indicate a phase lag between modeled and observed data, with all WRF-ADCIRC simulations peaking 3–4 h prior to observations (Figure 12a–c). It was hypothesized that the lag in the peak water levels was caused by the difference in the length of the simulations. To test the effect of the differences in initialization time of the meteorological forcing for the case of Hurricane Sandy, an additional simulation was performed with the same configurations as CTL but beginning on 28 October 0000 UTC. The phase lag observed between the WRF-ADCIRC simulations and the station observations of about 3–4 h, was also apparent for the shorter CTL simulation. However, time-series for this simulation indicate that the shorter time configuration causes overestimation of the maximum water elevation at all station locations. This overestimation is thought to be a product of abruptly adding a very large TC as meteorological forcing for ADCIRC (see Section 3.3).

These results from the shorter CTL simulation therefore indicate sensitivity to the initialization time of the meteorological forcing and points to the cause of the observed phase shift in the WRF-ADCIRC simulations. The shorter CTL simulation was performed for purposes of testing, and henceforth we will only refer to the original CTL simulation initialized on 23 October 0000 UTC. Furthermore, hurricane Sandy was a slow-moving TC and the sensitivity to initialization time could be heightened by this factor, as the effect of the winds acting on the surface and generating surge are longer lasting for slower storms. It would prove interesting to examine other cases and explore this sensitivity of the simulated storm tracks to initialization time.

To further understand the coupled model characteristics, we shifted all the WRF-ADCIRC time series by 3 h (Figure 12d–f) so that the peak water levels would coincide with observations. This allowed for a better assessment of the magnitude of the water level each simulation could capture. For evaluation purposes the Pearson correlation coefficient (ρ) and the root mean square error (RMSE) were calculated for each simulation (Table 4). The coefficients of correlation between shifted modeled and observed water level estimates ranged between 0.76 and 0.93. Although the CTL simulation underestimated the water elevation at all stations, the strongest correlations are observed for this simulation with an average across stations of 0.91. Following the CTL simulation, FWP12 had the highest correlation and lowest RMSE averaging to 0.82 and 0.46 m, respectively, for all stations. Similarly, the FWP4 simulation had an average correlation of 0.78 and average RMSE of 0.49 m. The SCT12-4 simulation had an average correlation of 0.80 for all stations, and generally underestimated the water levels, specifically near the time of landfall.

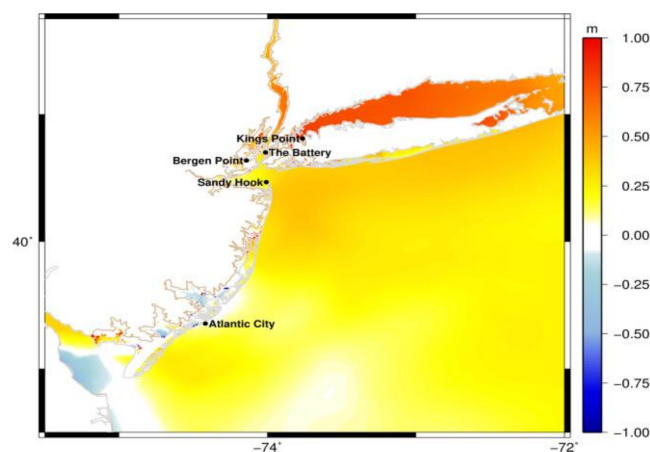


Figure 11. Difference in maximum water elevation between FWP12-4 and SCT12-4 (i.e., between track-forced simulation and the simulation forced with the full wind and pressure field output from WRF simulations of the same resolution).

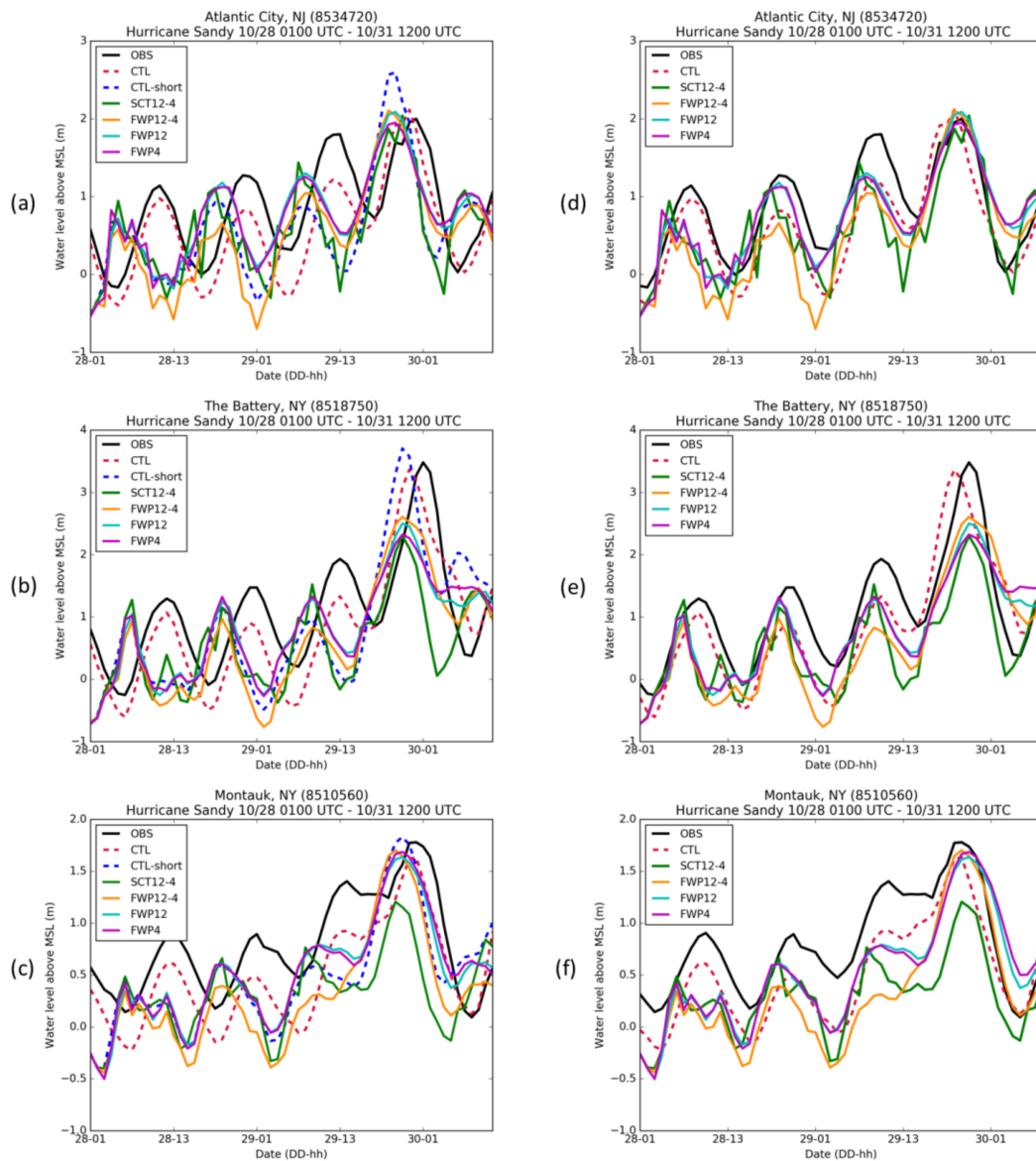


Figure 12. Times series of all simulations including a short CTL simulation for (a) Atlantic City NJ station; (b) The Battery NY station; and (c) Montauk NY station. The WRF-ADCIRC simulation estimates have been shifted by 3 h ahead of time to correspond with the peak of the observed water level and are shown for (d) Atlantic City NJ station; (e) The Battery NY station; and (f) Montauk NY station.

Investigation of the wind field structure for SCT12-4 shows that the wind radii estimates for the 34-, 50-, and 64-kt winds in the WRF12-4 km simulation are underestimated in comparison to wind structure data from the NHC-BT. These results highlight modeled storm surge sensitivity to wind structure and radii of maximum winds. The use of a track dataset, such as in SCT12-4, would rely on having accurate and consistent wind radii estimates. We should keep in mind that the NHC-BT data set is a post-storm analysis that uses various observational methods for assessment and reanalysis. On the contrary, the tracking algorithm used in this study to obtain track and wind radii estimates from the WRF simulation is based solely on the WRF model output. The incorporation of observations, as in NHC-BT, is omitted in SCT12-4 and can thus contribute to the errors discussed.

The FWP12-4 simulation usually estimated peaks that were lower in magnitude than both track-forced simulations: CTL and SCT12-4. However, near the time of landfall this pattern was altered. Although the water elevations for FWP12-4 remained lower than station observations, this simulation was able to capture the observed peak better than the SCT12-4 in all three stations (Figure 12d–f). Consideration should be given to the WRF 12-4 km simulation configuration. Near the time of landfall, the high-resolution vortex following nest (4 km) is positioned over the region where the stations are located. This pattern and the unexpected result of lower error in the SCT12-4 simulation implied that it may be a construct of including a moving nest in the WRF simulations, and of possible model grid interpolation problems. This hypothesis is further validated when we consider that the effect is minimized in Montauk station, which is the farthest station from the center of the TC and of the high-resolution domain.

Table 4. Statistics for water elevation of each simulation.

Simulation	Station	<i>p</i>	RMSE (M)
CTL	MTK	0.93	0.35
	BAT	0.89	0.52
	ACY	0.92	0.37
	Average	0.91	0.41
SCT12-4	MTK	0.81	0.58
	BAT	0.82	0.75
	ACY	0.76	0.51
	Average	0.8	0.61
FWP12-4	MTK	0.79	0.59
	BAT	0.8	0.77
	ACY	0.76	0.58
	Average	0.78	0.65
FWP12	MTK	0.8	0.43
	BAT	0.83	0.59
	ACY	0.82	0.37
	Average	0.82	0.46
FWP4	MTK	0.76	0.45
	BAT	0.79	0.64
	ACY	0.8	0.38
	Average	0.78	0.49

Figure 13 shows the wind vector output from ADCIRC for the CTL, SCT12-4, FWP12-4, FWP12 and FWP4 simulations for 29 October 2300 UTC. At the time of landfall, the CTL simulation shows the highest water level estimates in the NY Harbor among all five simulations (Figure 13a). The WRF-ADCIRC simulations exhibit lower water elevation estimates at landfall. In the CTL simulation, strong winds are angled perpendicular to the coast in the direction of the New York Harbor area. This is not the case for the WRF-ADCIRC simulations, where a combination of weaker northeasterly winds prevails in the New York Harbor coastal region. Results in Figure 13 also highlight the discrepancy in landfall timing, where the simulated TCs in the WRF-ADCIRC simulations make landfall after the observed time. This effect is more pronounced for the FWP4 simulation as observed in Figure 13e. Another important result illustrated in Figure 13 is the depiction of weaker winds over land for all the WRF-ADCIRC simulations. This difference in the wind field structure is not observed for CTL.

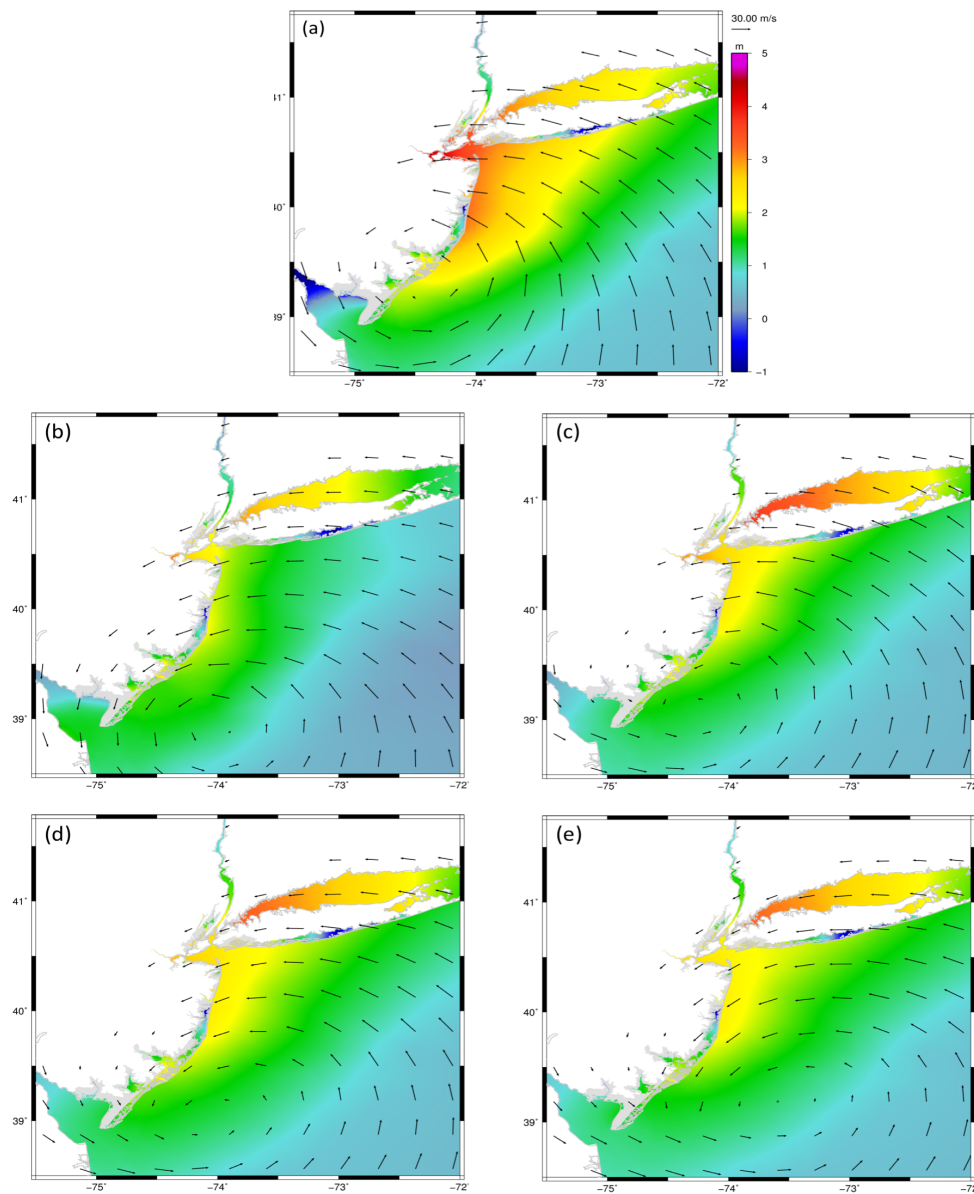


Figure 13. Maximum water elevation with ADCIRC wind vector output on 29 October 2300 UTC for (a) CTL; (b) SCT12-4; (c) FWP12-4; (d) FWP12; and (e) FWP4. The length of the 30 ms^{-1} wind vector is provided as reference.

4. Discussion

Accurate meteorological data is a critical factor in effectively capturing storm surge impacts. The simulated minimum pressure and winds from the WRF simulations corresponded well with station observations for Hurricane Sandy. However, discrepancies in wind speed were seen in some meteorological stations. The station time-series analysis however, presented some limitations. The corresponding station locations in WRF are given by the closest grid point to the station, and thus our results are not precise point-to-point comparisons. Errors in distance between the WRF station location with respect to their actual location ranged between 3.3 and 6.4 km for the New York Harbor Entrance and the Bergen Point stations.

Much of the error in the coupled WRF-ADCIRC simulations can be attributed to differences in the wind representation in each of the models. In terms of the maximum water elevation, generally, higher values are observed in areas right of the storm track, as is expected for TCs given their characteristic

right-of-track wind maximum pushing water ashore. ETCs however, as is the case for Hurricane Sandy, can exhibit wind maxima on both sides of the track. Given the angle at which Hurricane Sandy approached the coast near landfall, wind maxima to the left of the track forces more water away from the coast reducing the observed storm surge in the region south of landfall. This was the case for the WRF simulated TCs. Moreover, in the CTL simulation, as it was observed for Hurricane Sandy, the perpendicular direction of the winds on the right of the track, is allowing more water to be pushed onshore. As illustrated in Figure 13, this is not the case for the WRF-ADCIRC simulations. These results motivate the need to understand what the storm surge response would have been if the winds were to be weaker or stronger and directed in alternative angles. The response of storm surge to varying TC characteristics is the subject of ongoing research.

Results from our time-series comparisons indicate a phase lag between modeled and observed data, with all WRF-ADCIRC simulations peaking 3–4 h prior to observations (Figure 12a–c). This result is not uncommon, and it has been shown to occur in other studies. For example, Colle et al. [5], showed that in their WRF ensemble experiment, some members predicted peak storm surge up to 12 h too soon. In our case, the WRF simulations have a lag of their own with maximum winds peaking about 6 h prior to observations (Section 3.1). Part of this error is expected to propagate into the ADCIRC storm surge estimates. Moreover, Akbar et al. [15] discussed the effect of bottom friction as another potential source of error in storm surge simulations. Their results show early peak arrival for simulations with decreased bottom friction parameter and the opposite effect for increased bottom friction. Results from the CTL simulation, forced with NHC-BT data, do not exhibit the shift in peak arrival. It is worth highlighting the differences in initialization time of the meteorological forcing between the CTL simulation and the WRF-ADCIRC simulations. The CTL simulation was initialized on 23 October 0000 UTC, at the start of the NHC-BT record. To minimize errors in the simulated storm the WRF simulations were initialized 5 days after on 28 October 0000 UTC, and the atmospheric forcing in ADCIRC thus began at that time. Although the time evolution of the storm is important to capture the finer storm surge details at landfall, the track errors for simulations initialized prior to the chosen date had a left-of-track bias, as was also found by Galarneau et al. [19]. Studies have shown that for tracks that make landfall within 150 km of the observed landfall location, storm surge forecasts can be underestimated by 0.5–1.0 m [5]. Thus, we selected the configuration that minimized this error at landfall and best depicted the characteristics of Hurricane Sandy. In our simulations, the choice of initialization time seems to be the biggest factor influencing the shift in peak surge arrival.

Based on our results, we would rank (in decreasing order) the performance of our models as follows: CTL, FWP12, FWP4, SCT12-4 and FWP12-4. The time-series analysis showed that the CTL simulation forced with NHC-BT data compared well with observations, indicating a suitable ADCIRC model setup. This implies that we can reproduce accurate storm tide estimates with the best possible meteorological data available using a simplified parametric model. Yin et al. [33], found similar results in their storm surge assessment of Hurricane Sandy. Results showed the effectiveness of their simulation in accurately predicting the timing and magnitude of the peak surge. However, some discrepancies were observed before and after the peak surge, which they have attributed to the use of a simplified parametric vortex model for their wind field representation.

Time-series results from the WRF-ADCIRC simulations show discrepancies when compared to CTL. Discrepancies were more evident at The Battery, NY station where none of the WRF-ADCIRC simulations could accurately capture the magnitude of the peak storm surge (Figure 12e). Colle et al. [5], showed similar results of underestimated water levels for various of their WRF ensemble simulations. However, their control simulation which is most comparable in terms of configuration to our FWP12-4 simulation, captured the peak surge at The Battery. It overestimated the observed water elevations by 0.20 m. An important distinction between both studies is the implementation of wave coupling in their assessment, which has been neglected for the purposes of this study.

Statistical results in Table 4 indicate that the track-forced SCT12-4 simulation has a higher average correlation coefficient and lower average RMSE than the FWP12-4 simulation. However, simulations with meteorological forcing in the form of wind and pressure fields from full-physics atmospheric models are assumed to contribute less error than track-forced simulations that make use of parametric wind models. Parametric wind models can have between 10% and 20% higher random error [2], an assumption based on the fact that these do not account for details in the wind structure as atmospheric models do. Parametric wind models also fail to capture interactions with topography and TC dynamics and feedbacks, which are important in storm surge modeling. The FWP12 and FWP4 simulations show improvement over the track-based simulations, which leads us to conclude that the improvement of SCT12-4 over FWP12-4 is a construct of including a vortex-following nest in the WRF 12-4 km simulation. The sensitivity of storm surge simulations to atmospheric forcing resolution in the FWP simulations was also investigated. When comparing the FWP simulations, results indicate that for our case the coarser horizontal resolution simulation (WRF 12 km) is sufficient to forecast storm surge estimates and there is no need for increased resolution.

Although storm surge predictions from CTL can be considered as a standard for the real case, the values might be an overestimate, given the lack of interaction with topography acting to weaken the storm. In their study, Dietrich et al. [10] found similar results for simulations forced with NHC advisories and implemented within GAHM. The maximum wind speed for their simulation remained relatively constant at landfall and retained a larger wind field extent when compared to HWIND. The larger wind field caused higher water elevations for the track-based simulation. The weakening of winds caused by the interaction with land and topography, is evident in the FWP12-4 simulation, as shown by decreased wind speed over land in Figure 13c–d compared to CTL (Figure 13a). The methodology of directly extracting the TC properties used by the parametric models from the full-physics models can, to a certain degree, reduce this limitation by adding to the realism and complexity of the TC wind field. Moreover, these results point to the utility of using full physics models for forecasting storm surge. It implicitly accounts for weakening of winds and distortion of the wind field by the interaction with land.

The results of this study are not uncommon. Bennett and Mulligan [17] found that a 3D atmospheric model was more suitable for hindcasting the waves of Hurricane Sandy when compared to the Holland Model and the GAHM. However, one noticeable difference to our study is their use of an atmospheric model with data assimilation. A similar study by Dietrich et al. [10] highlighted the value in using parametric vortex models for hindcasting purposes but encouraged the use of full-physics coupled models for storm surge forecasting of Hurricane Isaac. Although results have been similar for various cases and geographic regions, the studies performed are location-dependent, thus prompting the need for a systematic study of the effect in the choice of atmospheric forcing.

5. Conclusions

In this study, we compare four WRF-ADCIRC simulations to determine the best choice in meteorological forcing for storm surge studies. For real-time forecasting of storm surge or in the absence of a best track data set, it is important to identify a suitable model configuration that can provide accurate atmospheric and surge forecasts. In this work, we explore ways of improving this modeling framework.

One of the simulations consisted of using track data estimated from a full-physics WRF 12-4 km simulation as meteorological forcing for the ADCIRC model. The GAHM was then implemented within the ADCIRC model to determine the wind field in the domain. The remaining three simulations directly used the full wind and pressure field output from the full-physics WRF 12-4 km, WRF 12 km and WRF 4 km simulations as meteorological forcing. All simulations were compared to a control run using the NHC-BT data for Hurricane Sandy.

Results indicate that our initial choice of meteorological forcing for estimating storm surge would depend on data availability. A best track data set appears to be the best meteorological forcing option

for our configuration of the ADCIRC model. However, when a best track is not available, our results would indicate that we could primarily rely on using full wind and pressure field output from a 12 km resolution WRF simulation.

The results of this study have encouraged the authors to further understand the sensitivity of storm surge impacts to atmospheric forcing and to varying storm characteristics. Ongoing research focuses on the sensitivity of storm surge to the track, intensity, and size of tropical cyclones in a coupled atmosphere, storm surge and wave modeling framework.

Acknowledgments: This material is based upon work supported by the National Science Foundation Graduate Research Fellowship Program under Grant No. DGE-1433187. Any opinions, findings, and conclusions or recommendations expressed in this material are those of the authors and do not necessarily reflect the views of the National Science Foundation. The authors also acknowledge the support of the National Science Foundation through Award OCE-1419584. This work was also supported in part by the School of Environmental and Biological Sciences and the Institute of Earth, Ocean, and Atmospheric Sciences at Rutgers University. We also want to acknowledge the National Center for Atmospheric Research's Advanced Study Program where part of the computing and research was conducted. Comments and suggestions from three anonymous reviewers and the editor greatly improved the quality of this manuscript.

Author Contributions: A.N.R.V., E.N.C. and C.L.B. conceived and designed the experiments; A.N.R.V. performed the experiments; A.N.R.V. and C.L.B. analyzed the data; C.L.B. and K.R.F. contributed reagents/materials/analysis tools; A.N.R.V. wrote the paper.

Conflicts of Interest: The authors declare no conflict of interest. The founding sponsors had no role in the design of the study; in the collection, analyses, or interpretation of data; in the writing of the manuscript, and in the decision to publish the results.

References

1. Smith, A.B.; Katz, R.W. US billion dollar weather and climate disasters: Data sources, trends, accuracy and biases. *Natl. Hazards* **2013**, *67*, 387–410. [CrossRef]
2. Resio, D.T.; Westerink, J.J. Modeling the physics of storm surges. *Phys. Today* **2008**, *61*, 33–38. [CrossRef]
3. Needham, H.F.; Keim, B.D.; Sathiaraj, D. A review of tropical cyclones: Data sources, trends, accuracy and biases. *Rev. Geophys.* **2015**, *53*, 545–591. [CrossRef]
4. Klotzbach, P.J.; Bowen, S.G.; Pielke, R., Jr.; Bell, M. Continental United States hurricane landfall frequency and associated damage: Observations and future risks. *Bull. Am. Meteorol. Soc.* **2018**. [CrossRef]
5. Colle, B.A.; Bowman, M.J.; Roberts, K.J.; Bowman, M.H.; Flagg, C.N.; Kuang, J.; Weng, Y.; Munsell, E.B.; Zhang, F. Exploring water level sensitivity for metropolitan New York during sandy (2012) using ensemble storm surge simulations. *J. Mar. Sci. Eng.* **2015**, *3*, 428–443. [CrossRef]
6. National Center for Environmental Information (NCEI). U.S. Billion Dollar Weather and Climate Disasters. Available online: <https://www.ncdc.noaa.gov/billions/> (accessed on 9 March 2018).
7. Blake, E.S.; Kimberlain, T.B.; Berg, R.J.; Cangialosi, J.P.; Beven li, J.L. Tropical cyclone report: Hurricane sandy. *Natl. Hurric. Cent.* **2013**, *12*, 1–10.
8. Hall, T.M.; Sobel, A.H. On the impact angle of hurricane Sandy's New Jersey landfall. *Geophys. Res. Lett.* **2013**, *40*, 2312–2315. [CrossRef]
9. Barnes, E.A.; Polvani, L.M.; Sobel, A.H. Model projections of atmospheric steering of sandy-like superstorms. *Proc. Natl. Acad. Sci. USA* **2013**, *110*, 15211–15215. [CrossRef] [PubMed]
10. Dietrich, J.; Muhammad, A.; Curcic, M.; Fathi, A.; Dawson, C.; Chen, S.; Luettich, R., Jr. Sensitivity of storm surge predictions to atmospheric forcing during hurricane ISAAC. *J. Waterw. Port Coast. Ocean Eng.* **2017**, *144*, 04017035. [CrossRef]
11. Lakshmi, D.D.; Murty, P.; Bhaskaran, P.K.; Sahoo, B.; Kumar, T.S.; Sheno, S.; Srikanth, A. Performance of WRF-ARW winds on computed storm surge using hydrodynamic model for Phailin and Hudhud Cyclones. *Ocean Eng.* **2017**, *131*, 135–148. [CrossRef]
12. Holland, G.J. An analytic model of the wind and pressure profiles in hurricanes. *Mon. Weather Rev.* **1980**, *108*, 1212–1218. [CrossRef]
13. Gao, J.; Luettich, R.; Fleming, J. Development and initial evaluation of a generalized asymmetric tropical cyclone vortex model in ADCIRC. In Proceedings of the ADCIRC Users Group Meeting, Vicksburg, MS, USA, 16 July 2013.

14. Mattocks, C.; Forbes, C.; Ran, L. *Design and Implementation of a Real-Time Storm Surge and Flood Forecasting Capability for the State of North Carolina*; UNC-CEP Technical Report; University of North Carolina: Chapel Hill, NC, USA, 2006; Volume 103.
15. Akbar, M.K.; Kanjanda, S.; Musinguzi, A. Effect of bottom friction, wind drag coefficient, and meteorological forcing in hindcast of hurricane rita storm surge using SWAN+ ADCIRC model. *J. Mar. Sci. Eng.* **2017**, *5*, 38. [[CrossRef](#)]
16. Powell, M.D.; Houston, S.H.; Amat, L.R.; Morisseau-Leroy, N. The HRD real-time hurricane wind analysis system. *J. Wind Eng. Ind. Aerodyn.* **1998**, *77*, 53–64. [[CrossRef](#)]
17. Bennett, V.C.; Mulligan, R.P. Evaluation of surface wind fields for prediction of directional ocean wave spectra during hurricane sandy. *Coast. Eng.* **2017**, *125*, 1–15. [[CrossRef](#)]
18. Skamarock, W.; Klemp, J.; Dudhia, J.; Gill, D.; Barker, D.; Duda, M.; Huang, X.; Wang, W.; Powers, J. *A Description of the Advanced Research WRF Version 3*, NCAR Technical Note, Mesoscale and Microscale Meteorology Division; National Center for Atmospheric Research: Boulder, CO, USA, 2008.
19. Galarneau, T.J.; Davis, C.A.; Shapiro, M.A. Intensification of hurricane sandy (2012) through extratropical warm core seclusion. *Mon. Weather Rev.* **2013**, *141*, 4296–4321. [[CrossRef](#)]
20. ECMWF. *Era-Interim Project. European Centre for Medium-Range Weather Forecasts: Research Data Archive at the National Center for Atmospheric Research*; Computational and Information Systems Laboratory: Boulder, CO, USA, 2009.
21. Hong, S.-Y.; Lim, J.-O.J. The WRF single-moment 6-class microphysics scheme (WSM6). *J. Korean Meteorol. Soc.* **2006**, *42*, 129–151.
22. Hong, S.-Y.; Noh, Y.; Dudhia, J. A new vertical diffusion package with an explicit treatment of entrainment processes. *Mon. Weather Rev.* **2006**, *134*, 2318–2341. [[CrossRef](#)]
23. Tiedtke, M. A comprehensive mass flux scheme for cumulus parameterization in large-scale models. *Mon. Weather Rev.* **1989**, *117*, 1779–1800. [[CrossRef](#)]
24. Iacono, M.J.; Delamere, J.S.; Mlawer, E.J.; Shephard, M.W.; Clough, S.A.; Collins, W.D. Radiative forcing by long-lived greenhouse gases: Calculations with the AER radiative transfer models. *J. Geophys. Res. Atmos.* **2008**, *113*. [[CrossRef](#)]
25. Chen, F.; Dudhia, J. Coupling an advanced land surface-hydrology model with the penn state-NCAR MM5 modeling system. Part I: Model implementation and sensitivity. *Mon. Weather Rev.* **2001**, *129*, 569–585. [[CrossRef](#)]
26. Luettich, R.A.; Westerink, J.J.; Scheffner, N.W. *ADCIRC: An Advanced Three-Dimensional Circulation Model for Shelves, Coasts, and Estuaries. Report 1. Theory and Methodology of ADCIRC-2DDI and Adcirc-3DL*; Coastal Engineering Research Center: Vicksburg, MS, USA, 1992.
27. Luettich, R.; Westerink, J. *Formulation and Numerical Implementation of the 2D/3D ADCIRC Finite Element Model Version 44*; University of North Carolina: Chapel Hill, NC, USA, 2004. Available online: http://www.unc.edu/ims/adcirc/adcirc_theory_2004_12_08.pdf (accessed on 3 April 2018).
28. Fossell, K.R.; Ahijevych, D.; Morss, R.E.; Snyder, C.; Davis, C. The practical predictability of storm tide from tropical cyclones in the gulf of Mexico. *Mon. Weather Rev.* **2017**, *145*, 5103–5121. [[CrossRef](#)]
29. Forbes, C.; Luettich, R.A., Jr.; Mattocks, C.A.; Westerink, J.J. A retrospective evaluation of the storm surge produced by hurricane gustav (2008): Forecast and hindcast results. *Weather Forecast.* **2010**, *25*, 1577–1602. [[CrossRef](#)]
30. Dietrich, J.; Bunya, S.; Westerink, J.; Ebersole, B.; Smith, J.; Atkinson, J.; Jensen, R.; Resio, D.; Luettich, R.; Dawson, C. A high-resolution coupled riverine flow, tide, wind, wind wave, and storm surge model for southern Louisiana and Mississippi. Part II: Synoptic description and analysis of hurricanes katrina and rita. *Mon. Weather Rev.* **2010**, *138*, 378–404. [[CrossRef](#)]
31. Lin, N.; Smith, J.A.; Villarini, G.; Marchok, T.P.; Baeck, M.L. Modeling extreme rainfall, winds, and surge from hurricane isabel (2003). *Weather Forecast.* **2010**, *25*, 1342–1361. [[CrossRef](#)]
32. Colle, B.A.; Buonaiuto, F.; Bowman, M.J.; Wilson, R.E.; Flood, R.; Hunter, R.; Mintz, A.; Hill, D. New York city's vulnerability to coastal flooding: Storm surge modeling of past cyclones. *Bull. Am. Meteorol. Soc.* **2008**, *89*, 829–841. [[CrossRef](#)]
33. Yin, J.; Lin, N.; Yu, D.P. Coupled modeling of storm surge and coastal inundation: A case study in New York city during hurricane sandy. *Water Resour. Res.* **2016**, *52*, 8685–8699. [[CrossRef](#)]

34. Cialone, M.A.; Grzegorzewski, A.S.; Mark, D.J.; Bryant, M.A.; Massey, T.C. Coastal-storm model development and water-level validation for the North Atlantic coast comprehensive study. *J. Waterw. Port Coast. Ocean Eng.* **2017**, *143*, 04017031. [[CrossRef](#)]
35. Lin, N.; Emanuel, K.A.; Smith, J.; Vanmarcke, E. Risk assessment of hurricane storm surge for New York city. *J. Geophys. Res. Atmos.* **2010**, *11*. [[CrossRef](#)]
36. Federal Emergency Management Agency (FEMA). *Region II Coastal Storm Surge Project: Mesh Development*; Federal Emergency Management Agency: Washington, DC, USA, 2014.
37. Orton, P.; Vinogradov, S.; Georgas, N.; Blumberg, A.; Lin, N.; Gornitz, V.; Little, C.; Jacob, K.; Horton, R. New York city panel on climate change 2015 report Chapter 4: Dynamic coastal flood modeling. *Ann. N. Y. Acad. Sci.* **2015**, *1336*, 56–66. [[CrossRef](#)] [[PubMed](#)]
38. Cangialosi, J.P.; Franklin, J.L. *Forecast Verification Report: 2016 Hurricane Season*; National Oceanic and Atmospheric Administrations (NOAA) National Hurricane Center (NHC): Miami, FL, USA, 2017.
39. NOAA/NOS/CO-OPS. Tides and Currents. Available online: <https://tidesandcurrents.noaa.gov/> (accessed on 8 November 2017).



© 2018 by the authors. Licensee MDPI, Basel, Switzerland. This article is an open access article distributed under the terms and conditions of the Creative Commons Attribution (CC BY) license (<http://creativecommons.org/licenses/by/4.0/>).